New Pressure Drop Correlation for Sieve Tray Distillation Columns

Pressure drop data for distillation sieve trays have been obtained with experimental trays with small outlet weir heights, including zero, and for trays with small perforations which exhibit large pressure drops due to surface tension. These data have been added to literature data to form a large composite data base with extensive variations in fluid and gas properties, flow rates, and tray designs.

A new pressure drop correlation has been developed which retains the use of the dry tray pressure drop, but provides new procedures for estimating liquid inventory and the resistance to vapor flow due to surface tension forces. This correlation gives a mean absolute error of 6.0% and an average error of −0.6%. These errors are significantly less than the errors between measurements and predictions from two other correlations using the same composite data base.

D. L. BENNETT, RAKESH AGRAWAL, and P. J. COOK

Process Systems Group
Air Products and Chemicals, Inc.
Allentown, PA 18105

SCOPE

Pressure drops across distillation column sieve trays should be estimated accurately as part of column designs to determine downcomer backup, column pressure drop, and tray efficiency. These pressure drop calculations become more important in designs for nonfouling service, where small tray spacings are used and flooding limits tray capacity.

The objectives of this paper are:

a. To determine whether the liquid inventory on a sieve tray can be measured by a tray-mounted manometer, or whether the inventory should be estimated from the total measured pressure drop by subtracting the other pressure drop components.

b. To report sieve tray pressure drop data from trays with low outlet weir heights, including zero, and for trays with small perforations which exhibit large surface tension pressure drops.

c. To develop a composite data base, consisting of the above data and literature data, which has large variations in fluid and gas properties, flow rates and tray designs.

d. To develop a simple pressure drop correlation for sieve trays based on this composite data base, and to compare the accuracy of this correlation with that of several other correlations, using the same data base.

CONCLUSIONS AND SIGNIFICANCE

Tray-mounted manometers had been suggested as possible tools for direct measurement of clear liquid head on aerated sieve trays. Time-average measurements made on special trays with fixed liquid inventories showed large discrepancies with known average liquid heads, dependent upon vapor flow rates and clear liquid heads. Therefore, clear liquid heads were determined from total pressure drop measurements from an independent evaluation of surface tension resistance and conventional dry hole pressure drops.

Pressure drop data are reported in Table 1 for trays with small weir heights and small perforation sizes. These data were added to literature data to develop a large composite data base with the extensive range of fluid and gas properties, flow rates, and tray designs summarized in Table 2.

A pressure drop correlation has been developed using this composite data base. The total pressure drop is assumed to consist of the dry tray component, the liquid inventory and the resistance to vapor flow due to surface tension forces.

The liquid inventory was correlated by defining an effective froth height which was shown to be a function of weir height and volumetric froth flow rate. Correlations of the effective froth density with a number of possible dimensionless groups were evaluated and a correlation relating the ratio of froth and liquid densities to the density corrected superficial velocity (K_s) was found to be most successful.

The vapor flow resistance due to surface tension forces has been correlated based on work requirements to generate interfacial area and a force balance at bubble departure. The correlation predicts that the surface tension pressure drop is inversely proportional to the cube root of the perforation diameter, rather than the first power as previously hypothesized.

These correlations, when used to calculate the total sieve tray pressure, give an average error for the composite data base of −0.6% with a standard deviation of 7.8%. The mean absolute error is 6.0%. These errors are significantly less than errors exhibited by two other correlations when compared with the same composite data base.

INTRODUCTION

Distillation sieve tray pressure drop measurements have been reported by a number of investigators. Foss and Gerster (1956) reported one of the first comprehensive studies of sieve trays. They studied 4.7-mm perforated trays with open areas ranging from 4.2 to 10.6%. The outlet weir heights were 25, 50, and 100 mm. Air/water pressure drop measurements were also reported by Friend et al. (1960), who studied 4.76-, 9.5-, and 12.7-mm perforated trays, with open areas of 7.8, 9.6, and 12.2%. They tested trays with 0-, 25-, and 50-mm-high outlet weirs. Lemieux and Scotti (1969) and Nutter (1971) also report air/water results. Lemieux and Scotti tested trays with a 25-mm outlet weir and 12.7- and 25-mm perforations. The tested open area was 7.4, 9.6, and 10%. Nutter's (1971) data were taken in a 12.7-mm perforated tray with a 50 mm outlet weir and 7.9% open area.

0001-1541-83-6811-0434-$2.00.

TABLE 1. TOTAL PRESSURE DROP DATA FOR 0.152 × 0.61 m² SIEVE TRAYS

		For 1-mm Hole Tray		For 3-mm Hole Tray	
V_s	h_w	$Q \times 10^2$	h_T	$Q \times 10^2$	h_T
m/s	(m)	(m^3/min)	(m)	m^3/min	(m)
0.8636	0	1.363	0.0399		
0.7620	0	1.817	0.0406		
0.6604	0	2.877	0.0417		
1.0160	0.0032	0.681	0.0371		
0.8636	0.0032	1.363	0.0396		
0.5080	0.0032	1.817	0.0406		
0.4064	0.0032	2.877	0.0411		
0.8890	0.0064	0.681	0.0376		
0.4064	0.0064	1.363	0.0401		
0.3556	0.0064	1.817	0.0406		
0.1524	0.0064	2.877	0.0414		
0.6604	0.0095	0.681	0.0381		
0.3556	0.0095	1.363	0.0411		
1.0160	0			1.817	0.0351
0.8636	0			2.877	0.0356
1.4224	0.0032			1.817	0.0351
1.0160	0.0032			2.877	0.0356
1.4224	0.0064			1.363	0.0356
1.2700	0.0064			1.817	0.0358
1.0160	0.0064			2.877	0.0361
1.1176	0.0095			1.363	0.0356
0.9144	0.0095			1.817	0.0356
0.7620	0.0095			2.877	0.0361
1.4224	0.0127			1.817	0.0361
0.9144	0.0127			2.877	0.0366
1.3970	0.0191			1.363	0.0366
0.9144	0.0191			1.817	0.0371
0.7620	0.0191			2.877	0.0371
1.2700	0.0254			0.681	0.0361
0.8890	0.0254			1.363	0.0366
0.6350	0.0254			1.817	0.0366
0.6350	0.0254			2.877	0.0371

TABLE 2. VARIATION IN PROPERTIES OR FLOWS FOR SETS OF DATA USED IN COMPOSITE DATA BASE

Parameter	Min. Value	Max. Value	Ratio of Max. to Min. Values
K_s	0.0052	0.1219 m/s	23
Q_L	0.0447	1.6390 m^3/m·min	37
h_W	0.0	0.1016 m	—
D_H	1	25.4 mm	25
ρ_L	433	1,000 kg/m^3	2.3
ρ_V	1.1218	52.08 kg/m^3	46
σ	0.0025	0.0719 N/m	29
μ	6.5×10^{-5}	2.3×10^{-3} N·s/m^2	35
Total Data Points		300	302
Total Sources		8	8

Little nonair/water data are available. Nutter (1979) reports isopar-m oil and air data for a 12% open area tray with 12.7-mm perforations. He reports data from trays with 38- and 50-mm outlet weirs. Sakata and Yanagi (1979) report cyclohexane/n-heptane and isobutane/n-butane data under distillation conditions. These tests used a 12.7-mm perforated tray with an 8.2% open area and a 50-mm outlet weir.

The sieve tray pressure drop data reported in the above references are reasonably comprehensive with the exception that there are no data taken with outlet weirs between zero and 25 mm, and all the reported data have large tray perforations which result in small vapor resistance to flow due to surface tension forces, h_σ.

EXPERIMENTAL PROGRAM

Data have been obtained for trays with small outlet weir heights ranging from zero to 25 mm, and with tray designs exhibiting large surface tension pressure drop.

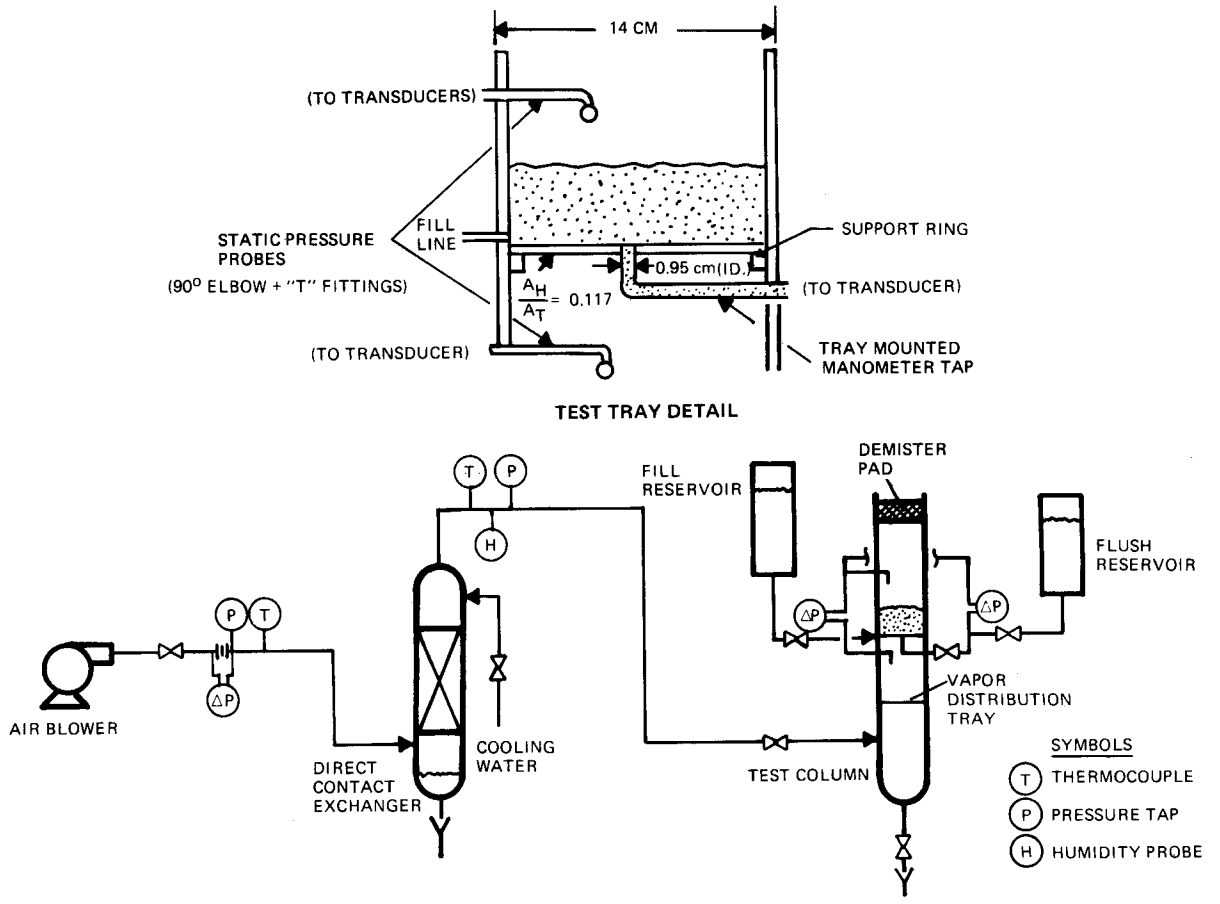

Figure 1. Test apparatus for evaluation of tray mounted manometer and determination of h_σ.

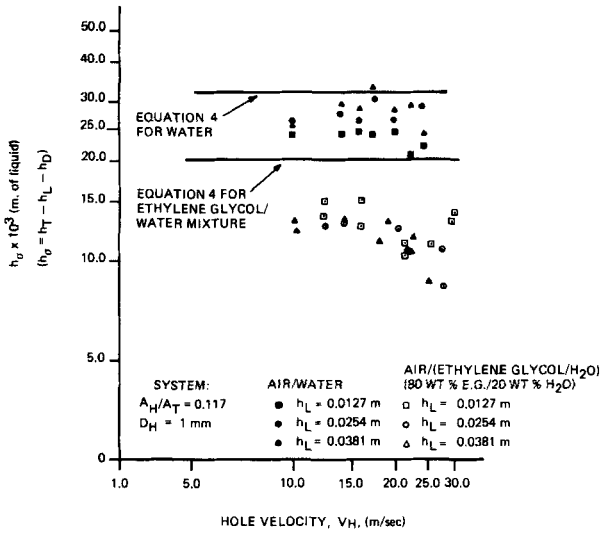

Figure 2. Experimental surface tension pressure drop component, h_σ, for an active sieve tray.

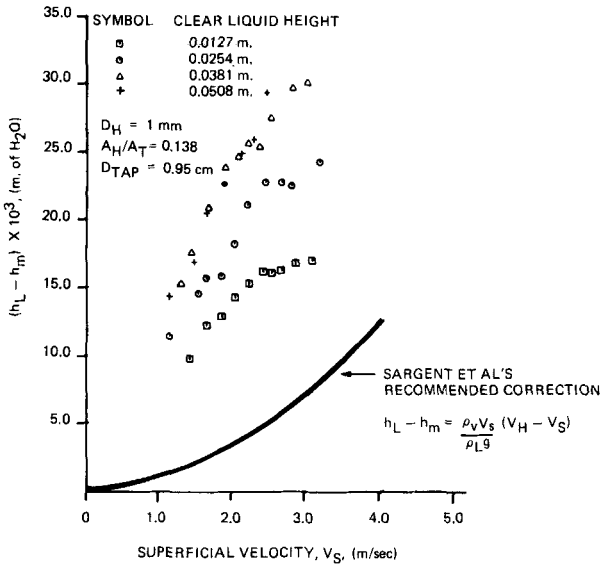

Figure 3. Difference between actual liquid height, h_L, and tray mounted manometer reading, h_m, for an active sieve tray.

Prior to conducting these tests, a preliminary program was required to determine whether tray-mounted manometers accurately measure the liquid inventory on the tray, h_L, or whether h_L is better determined from the total pressure drop. In Figure 1, the apparatus used to investigate h_L measurements from tray-mounted manometers is illustrated. This equipment was also used to determine experimental h_σ values.

The air from the blower was measured with an annubar and saturated and cooled with water in a packed bed. Temperature, pressure and humidity were measured prior to entering the test column. The inlet air impacted the curved bottom cap of the apparatus and passed through a dummy tray to improve flow uniformity. A known quantity of water was charged onto the test tray prior to each set of air/water tests. The liquid inventory was checked after each run by shutting down the air supply and measuring the liquid head on the tray with the tray-mounted manometer and checking this value against the measured liquid height.

Two manometers were attached flush with the top surface of the tray. One was located on the centerline, and the other one-half of the radius from the centerline. These manometers were attached to a Validyne Engineering Corp. Model: PD-15-42 transducer, and the transient response was displayed on an Esterline-Angus recorder. The line from the transducer to the tray floor was flushed with water prior to a reading, to remove any bubbles in the line.

Total tray pressure drop was also recorded, and the dry tray pressure drop was evaluated for each sieve tray tested. To increase h_σ, a very small perforation diameter of about 1 mm was selected. Additional tests were also carried out with a perforation diameter of about 3 mm.

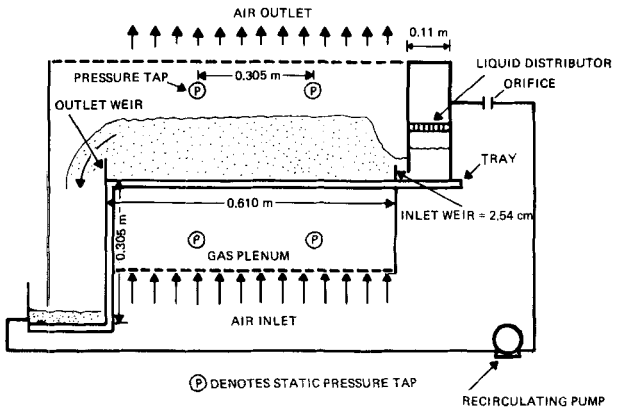

Figure 4. Experimental apparatus to study the effects of small weirs.

By assuming that the resistance to vapor flow through the wetted perforations, h_V, is equal to the dryhole value, h_D,h_σ can be determined from $h_T - h_D - h_L$, where h_L is the measured clear liquid head. In Figure 2, these experimental air/water h_σ values are plotted against hole velocity. Also plotted are predictions based on Sterbacek's equation (Eq. 4). The experimental values appear to be insensitive to vapor rate, and only slightly dependent upon h_L. Tests with air/ethylene glycol, which exhibit lower surface tension resistance to flow than to tests with air/water, also show the same trend and also show that the experimental h_σ values are significantly less than those predicted from Eq. 4. According to Eq. 4, h_σ is inversely proportional to D_H, however, the h_σ values for the tray with 3-mm perforations are only about 0.6 of the 1 mm hole diameter values, indicating a smaller dependency on D_H than Eq. 4 indicates.

In Figure 3, the measured tray-mounted manometer value, h_m, for the air/water tests, is subtracted from the known h_L value and plotted vs. superficial gas velocity. Sargent et al. (1964) reports that the values for h_m and h_L are not identical and must be corrected by the gas momentum change. His recommended correction factor is also plotted in Figure 3. The difference between h_m and h_L appears to be almost linear with respect to vapor rate, and a strong function of both the vapor rate and h_L. Furthermore, the value for $h_L - h_m$ is about three times the value determined solely by a momentum balance. The magnitude of this discrepancy is consistent with the results reported by Thomas and Ogboja (1978). The reasons for these differences may be attributed to acceleration and energy losses of the vapor as the vapor passes through the perforation and froth layer. These tests show that measurements of h_L by a tray-mounted manometer are difficult, and require significant empirical correction prior to use. Therefore, estimating h_L from $h_T - h_D - h_\sigma$ values is more accurate and was used for this study.

In Figure 4, the experimental apparatus used to determine the effects of small weirs is shown. Air passed from a blower through a gas plenum and through the tray perforations. Water was pumped through an orifice plate and onto a distributor in the downcomer. The outlet weir length was 0.152 m. Two sieve trays with hole sizes of 1 mm and 3 mm were studied. The experimental results are given in Table 1 for each weir height and flow combination.

CORRELATION DEVELOPMENT

Review of Other Correlations

Most correlations attribute total tray pressure drop to three factors which contribute resistance to vapor flow. These factors are: the liquid inventory on the tray, the passage of the vapor through the perforations, and the formation of vapor bubbles. It has been customary to express pressure drop in terms of height of liquid on the tray; thus,

$$h_T = h_L + h_V + h_\sigma. \tag{1}$$

Most correlations assume that h_V is equal to the vapor flow resistance of the dry tray, h_D. This hypothesis can be challenged because of the vastly different vapor flow conditions for a wet tray, compared with a dry tray, including variations in flow through individual perforations, and liquid entrainment from the tray

below. However, this convention has worked well and will be retained in this paper. This assumption makes it possible to develop a separate correlation for h_σ, which cannot be measured separately. h_D is usually correlated by,

$$h_D = \frac{a}{{c_V}^2}\frac{\rho_V V_H^2}{\rho_L g}, \tag{2}$$

where c_V is a function of percent open area and the ratio of the perforation diameter to the tray thickness. The most popular correlations for a and c_V are given by Liebson et al. (1957).

Many different approaches for correlating h_L have been used. In 1950, Robinson and Gilliland recommended that h_L be estimated from,

$$h_L = h_{ow} + h_w + {}^1/_2 h_g$$

where h_{ow} is calculated by the Francis weir equation,

$$h_{ow} = C_F(\dot{Q}_L)^{2/3}. \tag{3}$$

A number of early authors, including Kemp and Pyle (1949), Hutchinson et al. (1949), Mayfield et al. (1952), and Fair (1963), recognized that the Robinson and Gilliland equation for h_L overestimates h_L. The method proposed by Fair (1963) is commonly used. He defined β, such that,

$$h_L = \beta h_{L\,\text{only}}$$

where $h_{L\ \text{only}}$ equals the liquid height on the tray if the liquid is unaerated and no weeping or entrainment occurs. Therefore, using the Francis weir equation,

$$h_{L\text{only}} = h_{ow} + h_w.$$

Fair estimated β from relative froth density (ϕ_a) data obtained by Foss and Gerster (1956), and a relationship between β and ϕ_a derived by Hutchinson et al. (1949). Fair plotted β against $\rho_V V_s^2$, and a reasonable curve fit from this plot is,

$$\beta = 0.58 + 0.42\ \text{Exp}(-1.62\rho_V{}^{1/2}V_s).$$

In 1967, Sterbacek suggested that the volumetric flow rate of the froth, instead of the liquid, should be used in the Francis weir equation. Therefore, the observed froth height on the tray is,

$$h_{Fa} = h_w + C_F\left(\frac{\dot{Q}_L}{\phi_a}\right)^{2/3} + \frac{1}{2}h_g$$

and

$$h_L = \phi_a h_{Fa}.$$

Sterbacek also recommends that h_σ be evaluated by,

$$h_\sigma = \frac{4_\sigma}{g\rho_L D_H}. \tag{4}$$

Sterbacek evaluated ϕ_a from the ratio of h_L, obtained by subtracting h_D from h_T, to the observed froth height h_{Fa}. He reports that his equation for h_L agrees with his experimental h_L values to within ±12% if he uses the observed ϕ_a value. Unfortunately, Sterbacek gives no correlation for ϕ_a or h_{Fa}.

In 1979, Colwell utilized a similar model. His equation is,

$$h_L = \phi_a\left[h_w + C_1\left(\frac{\dot{Q}_L}{\phi_a}\right)^{2/3}\right]. \tag{5a}$$

Colwell generated an equation for ϕ_a evaluated from the observed froth height and h_L values reported by Foss and Gerster (1956), Bernard and Sargent (1966), Nutter (1971), Duehler and Van Winkle (1969), and Harris and Roper (1962). His equation, which was based on energy analyses by Azbel (1963) and Kim (1966), is

$$\phi_a = \frac{1}{1 + 12.6\left[\frac{K_s^2}{gh_L}\right]^{0.4}\left(\frac{A_H}{A_T}\right)^{-0.25}} \tag{5b}$$

Using Eqs. 5a and 5b, Colwell derived an equation for C_1 based on calculations from air/water data of Foss and Gerster (1956), Brambilla et al. (1969) and Gilbert (1959). Colwell's correlation is,

$$C_1 = \frac{47.63}{Cd^{2/3}} \tag{5c}$$

where

$$Cd = 0.61 + 0.08\left(\frac{h_{Fa} - h_w}{h_w}\right) \text{ if } \frac{h_{Fa} - h_w}{h_w} < 8.135$$

or

$$Cd = 1.06\left(\frac{h_{Fa}}{h_{Fa} - h_w}\right)^{1.5} \text{ if } \frac{h_{Fa} - h_w}{h_w} > 8.135.$$

Colwell used Eqs. 5a, 5b and 5c to predict h_L and compared these predictions with experimental h_L values for a number of data bases. For the composite data base which he used to determine Eq. 5c, and his own air/water data the mean error is about 7%. For the data sets which he did not use to determine Eq. 5c, which include all nonair/water data bases, mean errors between 12 and 15% are reported.

Generation of Composite Data Base

A composite data base was generated from eight literature sources and the data for small exit weirs taken in the 0.152 m × 0.61 m apparatus. The eight literature works are Foss and Gerster (1956), Friend et al. (1960), Lemieux and Scotti (1969), Billet et al. (1969), Nutter (1971), Jones and Jones (1975), Nutter (1979), and Sakata and Yanagi (1979). Two sets of data were excluded from the last reference. For these two sets, all correlations predict pressure drops 50 to 60% higher than these reported values. The test conditions were for very low vapor rates and full aeration was unlikely. In Table 2, the range in properties, flows, and designs is given for the entire data base. As can be seen, pertinent parameters varied over an extensive range. The composite data base consists of 300 sets of data taken by eight groups of investigators.

Model for h_L Correlation

In Figure 5, some of the parameters to develop this new correlation are defined. The two-phase region above the tray can be divided into liquid continuous and vapor continuous regions. In the vapor continuous region, a lower liquid content region exists near the underside of the tray above. Droplets in this region will be carried upward by vapor drag. A higher liquid content, vapor continuous region also exists containing larger liquid fragments thrown into the vapor space. These fragments are too heavy to be carried to the upper tray by the superficial gas velocity. The combined height of the liquid continuous region and the higher liquid content region is designated $h_{2\phi}$, and contains essentially all of the liquid mass.

An effective relative froth density, ϕ_e, and effective froth height, h_{Fe}, are defined by,

$$h_{Fe}\phi_e = h_L = \frac{1}{\rho_L}\int_0^{h_{2\phi}} \rho_{2\phi}(z)dz \tag{6a}$$

and

$$h_{Fe} - h_w = C\left(\frac{\dot{Q}_L}{\phi_e}\right)^{2/3} \tag{6b}$$

These equations can be rearranged to give,

$$h_L = \phi_e\left[h_w + C\left(\frac{\dot{Q}_L}{\phi_e}\right)^{2/3}\right] \tag{7}$$

This equation is very similar to Sterbacek's and Colwell's expressions for h_L except that visual observations are not used to evaluate the relative froth density; Eqs. 6a and 6b are used instead. This is an important distinction between this work and previous studies. Because visual froth height measurements (h_{Fa}) are not required for Eq. 7, the large errors associated with these measurements at realistic vapor rates are not introduced into the correlation for the pressure drop.

The effective froth height, h_{Fe}, is expected to be similar to the height of the liquid continuous region. However, because of density

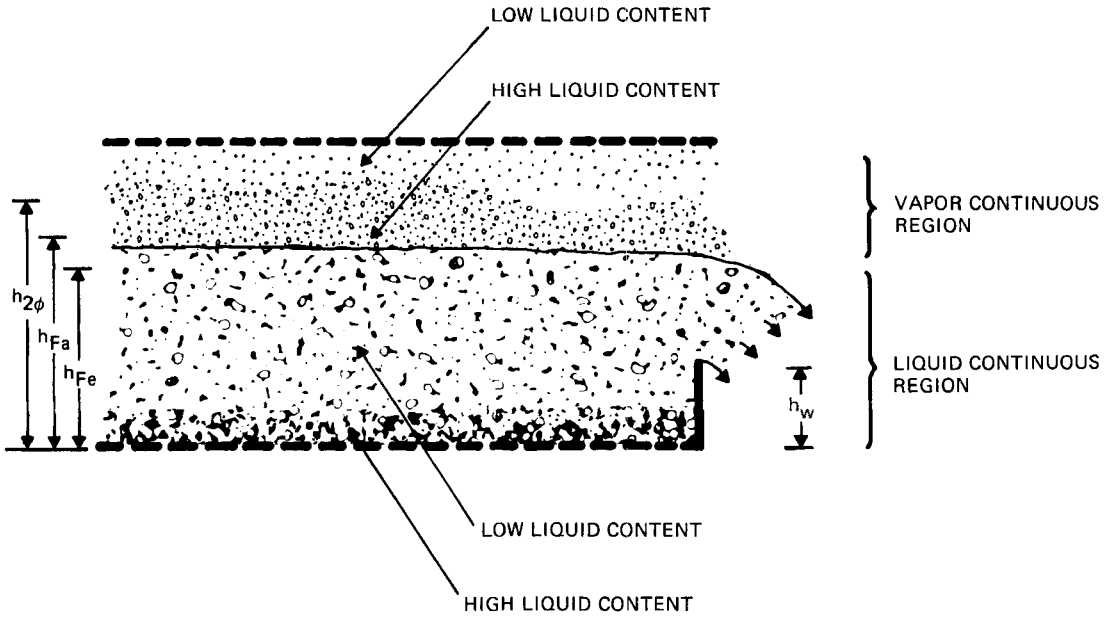

Figure 5. Froth model for h_L correlation.

gradients in the two-phase region, they will not be equivalent, and h_{Fe} can be significantly less than $h_{2\phi}$.

Equation 6b, in addition to Sterbacek's and Colwell's expressions, assumes that the crest of a froth over a weir is proportional to the volumetric flow rate per unit length of weir raised to the $\frac{2}{3}$ power. In the Appendix, an analysis is presented to investigate the $\frac{2}{3}$ power relationship, and the dependency of the constant C on geometry and assumptions. The analysis applies the Bernoulli equation along a streamline and the continuity equation across the stream tube. Two basic cases are analyzed. In Case 1, the force on the exit weir is assumed equal to only the hydrostatic force. In Case 2, the force is assumed equal to the sum of the hydrostatic force plus the impact force.

The Francis weir equation is usually restricted to conditions where the weir height is very large compared to the crest height. In Figure 6a, the calculated crest heights for Case 1 and Case 2, based on the equations in the Appendix, are plotted versus the volumetric flow rates per unit length of weir. The Francis equation is also plotted. Case 2 and Case 1 bound the Francis equation and all solutions exhibit the $\frac{2}{3}$ power dependency on flow rate. Case 2 appears more accurate for single-phase flow.

Calculated values for C, based on the analysis given in the Appendix, are plotted in Figure 6b, vs. h_w/h_f. Also plotted is the Francis weir coefficient, and the Rehbock equation (1929), which is recommended for single-phase flow when the crest is comparable to the weir height. All relationships approach a constant value as h_w/h_f goes to unity, i.e. when the crest is small compared to the weir height.

Pertinent Dimensionless Groupings for ϕ_e and C

The weir coefficient C and the effective relative froth density ϕ_e are required to determine h_L from Eq. 7.

C may be a function of density variations in the froth in addition to the ratio h_w/h_{Fe}. If C is assumed to be a function of h_{Fe}, an iterative solution of Eq. 7 is required. To avoid this, and because C is expected to be relatively constant, it was assumed that C is only a function of weir height.

Azbel (1963) and Colwell (1979) correlated relative froth density (ϕ_a) values versus a Froude number containing h_L for the characteristic length. This parameter is the ratio of the vapor inertial force to the gravity force acting on the froth. Since h_L is the unknown, an iterative solution of the ϕ_a equation is required.

Another approach also gives the Froude number as the appropriate dimensionless grouping; however, a different length parameter falls out. Imagine a bubble with radius r_B which ruptures near the top of the froth. A droplet with radius r_D is formed which contains a fraction δ of the fluid which formed the liquid membrane making up the bubble. The mass balance is,

$$r_D = \delta^{1/3}\phi^{1/3}r_B.$$

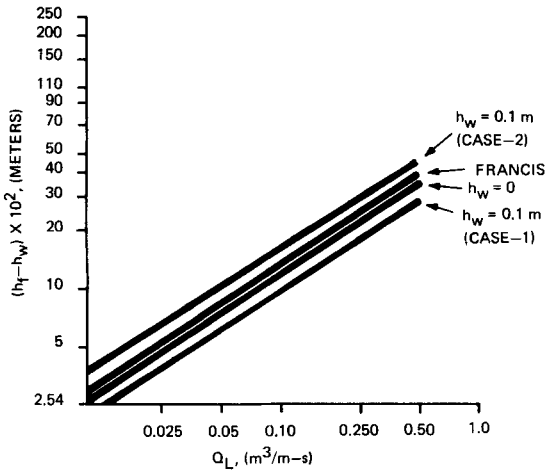

Figure 6a. Calculated results for the flow over the weir—assuming the fluid is of the uniform density.

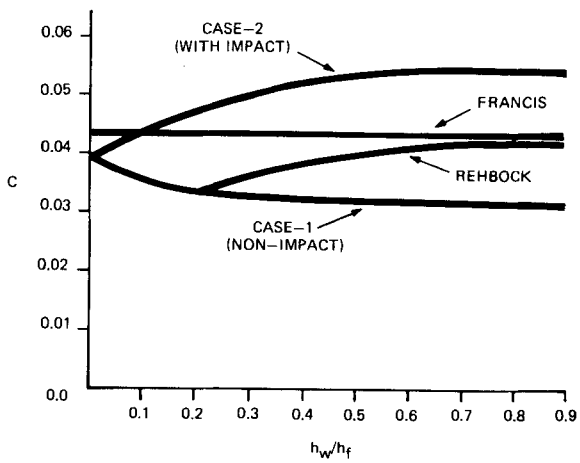

Figure 6b. Calculated constant C for the various cases.

Combining this with a force balance on the droplet with radius r_D gives,

$$\phi^{1/3}(1-\phi)^2 = \frac{6C_D}{g\delta^{1/3}}\frac{K_s^2}{D_B}$$

As K_s increases, the lefthand side increases. For ϕ ranging from 0 to 1.0, ϕ decreases as the lefthand side (or K_s) increases as required. C_D' and δ are unknown. Therefore, the above could be generalized to

$$\phi_e = f\left(\frac{K_s^2}{gD_B}\right).$$

Bhavaraju et al. (1978) have correlated bubble diameters in a sparge system versus a complicated liquid circulation Reynolds number. They report that for liquid circulation Reynolds numbers greater than 2,000, the characteristic bubble size reaches an asymptotic value of 0.0045 m, which is an experimental equilibrium diameter due to breakup and coalescence. All of the data included in the composite data base give circulation Reynolds numbers much greater than 2,000. Therefore, D_B may be constant. If this is true, or if D_B is only a function of K_s, ϕ_e would be only a function of K_s.

A number of additional Froude numbers can be defined and their accuracies in correlating the pressure drop data will be summarized later.

Model for h_σ

The pressure inside a bubble is greater than the ambient pressure and decreases as the bubble size increases. Pavlov (1964) determined the average pressure difference during the growth of a spherical bubble, by assuming liquid inertial effects are negligible. His equation is,

$$\Delta\bar{P}_B = \frac{6\sigma}{D_{B\max}} \tag{8}$$

$D_{B\max}$ should be controlled by a force balance at departure. Assuming a spherical bubble is attached to the perforation circumference and equating buoyancy and surface tension forces in the vertical direction, $D_{B\max}$ is calculated from,

$$D_{B\max} = b\left[\frac{D_H\sigma}{g(\rho_L-\rho_V)}\right]^{1/3} \tag{9}$$

where b equals $(6\sin\theta)^{1/3}$. Since b is expected to depend on θ, which is a function of the liquid and vapor properties, and the tray material, b must be evaluated experimentally.

Analysis of Data to Evaluate Correlations for h_L

The correlation for h_L is assumed to have the following format,

$$h_L = \phi_e\left[h_w + C\left(\frac{\dot{Q}_L}{\phi_e}\right)^{2/3}\right] \tag{10a}$$

For Eq. 10a, correlations for the weir coefficient C and the effective relative froth density ϕ_e are required.

The format assumed for the C correlation is,

$$C = a_1 + a_2\mathrm{EXP}[-a_3h_w]. \tag{10}$$

This equation will approach a constant value as h_w increases; however, C can either increase or decrease as h_w approaches zero.

The assumed functionality for ϕ_e is,

$$\phi_e = \mathrm{Exp}[-a_4(\pi_1)^{a_5}(\pi_2)^{a_6}] \tag{10c}$$

where π_1 is a parameter containing in part K_s, and π_2 is an additional parameter containing physical design differences. This format for Eq. 10c is very similar to Azbel's and Colwell's equation for ϕ_a since, $\mathrm{Exp}(-n)$ is approximately $1/(1+n)$, for small values of n.

Various choices of π_1 and π_2 were tested in Eq. 10c. These results are summarized in Table 3. Values of h_L were estimated by subtracting h_D and h_σ from the experimental values of h_T. Reported values for h_D or the Liebson et al. (1957) correlation were used to obtain h_D. For sets of data with significant h_σ values, experimental h_σ values were used. Values for a_1 through a_6 which minimize the standard deviation are tabulated in addition to the resultant average error and the mean absolute error. As indicated in this table, the most successful correlating parameter is K_s alone. This may suggest that the pertinent dimensionless grouping is the vapor Froude number using the froth bubble diameter as the characteristic dimension; for example,

$$\phi_e = f\left(\frac{K_s^2}{gD_B}\right)$$

with D_B essentially a constant. This would be consistent with the observations of Bhavaraju et al. (1978).

The coefficients which minimize the standard deviation give the following equations for C and ϕ_e,

$$C = 0.0327 + 0.0286\ \mathrm{EXP}[-137.8h_w(m)]$$
$$\phi_e = \mathrm{EXP}[-12.55(K_s(\mathrm{m/s}))^{0.91}]$$

TABLE 3. DIFFERENT POSSIBLE GROUPINGS FOR ϕ_e

π_1	π_2	$a_1\times10^2$	$a_2\times10^2$	a_3	a_4	a_5	a_6	Avg. Error (%)	Mean Abs. Error (%)
$\frac{K_s}{h_L^{1/2}}$	—	2.115	3.886	51.2	1.76	0.68	—	−5.24	9.44
$\frac{K_s}{(h_f-h_w)^{1/2}\phi_e^{1/2}}$	—	1.654	3.299	−92.1	0.63	0.785	—	68.54	68.81
$\frac{K_s}{D_H^{1/2}}$	—	3.434	2.892	120.1	0.86	0.355	—	−2.34	9.65
$\frac{K_s}{(\sigma/\mu)}$	—	−0.064	4.970	1425.2	*	*	—	5.0	18.4
$\frac{K_s}{D_H^{1/2}}$	$\frac{A_H}{A_T}$	2.530	3.253	145.7	2.01	0.49	0.34	−5.3	10.44
$\frac{K_s}{h_L^{1/2}}$	$\frac{D_H}{h_L}$	2.350	3.976	64.6	1.87	0.63	0.045	−5.3	9.49
$\frac{K_s}{h_L^{1/2}}$	$\left(\frac{A_H}{A_T}\right)$	2.530	3.976	74.0	1.31	0.715	−0.16	−5.6	9.6
K_s	—	3.272	2.865	137.8	12.55	0.91	—	−0.6	6.0

% Error = 100.0 (Calculated h_T − Experimental h_T)/(Calculated h_T).
Average Error = (Σ% error)/number of data points.
Mean Absolute Error = (Σ|% error|)/number of data points.

TABLE 4. ERRORS (AVERAGE, MEAN ABSOLUTE)*

Correlation	Data Bases: Nonair/Water		Air/Water		Total	
Colwell's (1979)	−4.5%	11.6%	−8.4%	10.3%	−7.4%	10.6%
New Correlation	2.4%	7.0%	−1.7%	5.6%	−0.6%	6.0%
Fair's (1963)	15.4%	15.7%	4.2%	9.5%	7.0%	11.0%

+ Errors = Calculated higher than experimental value.
− Errors = Calculated lower than experimental value.
*Errors are defined in Table 3.

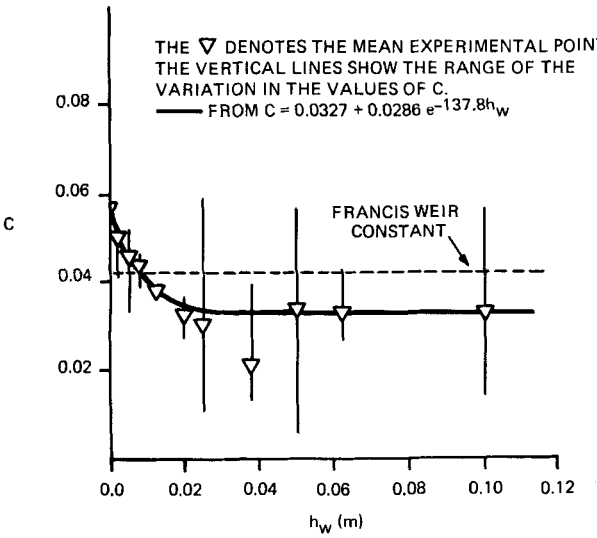

Figure 7. Experimental froth weir coefficient as a function of weir height, h_w.

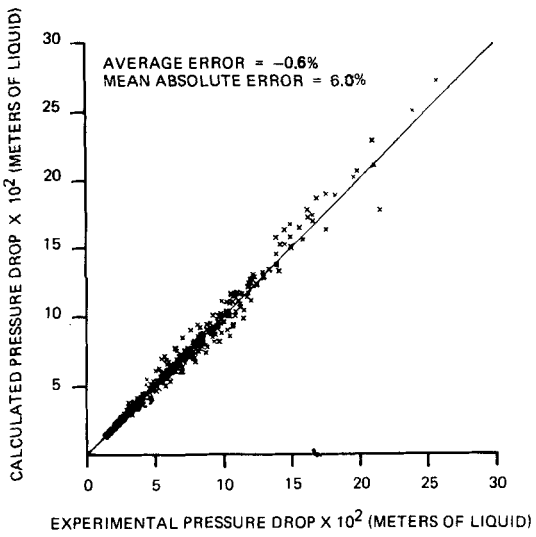

Figure 8. Calculated values of total pressure drop, h_T, using this new correlation compared against experimental values of h_T.

Discussion of Correlation

This new correlation for h_T assumes,

$$h_T = h_L + h_D + h_\sigma$$

where h_D behaves as indicated in Eq. 2 and either a and c_V are evaluated experimentally, or if required, from Liebson et al. (1957). h_L is obtained from,

$$h_L(m) = \phi_e \left[h_w(m) + C \left(\frac{\dot{Q}_L}{\phi_e} \right)^{2/3} \right]$$

where

$$C = 0.0327 + 0.0286\,\mathrm{EXP}[-137.8 h_w(m)]$$

$$\phi_e = \mathrm{EXP}[-12.55(K_s\ (\mathrm{m/s}))^{0.91}]$$

The correlation for h_σ is,

$$h_\sigma = \frac{6_\sigma}{g\rho_L D_{B\max}} \qquad (11a)$$

where

$$D_{B\max} = b \left[\frac{D_H \sigma}{g(\rho_L - \rho_V)} \right]^{1/3}$$

b should be evaluated from data, or estimated from $b = (6 \sin\theta)^{1/3}$. For air/water and air/ethylene glycol systems, θ equal to 20° appears reasonable; therefore, b equals 1.27.

In contrast to Eq. 4, this approach predicts that h_σ is inversely proportional to $D_H{}^{1/3}$. This agrees favorably with the experimental 1- and 3-mm perforation diameter h_σ data.

In Figure 7, the "experimental" values for C are plotted vs. h_w. Also plotted is the recommended correlation for C. The value for C approaches 0.0327 as h_w increases. This value is very close to the 0.0316 asymptote calculated for the nonimpact, or Case 1 example, as seen in Figure 6b. The data also suggest that C increases as h_w decreases, again in agreement with Case 1. However, the data indicate a larger increase in C than the predictions from the equations in the Appendix.

In Figure 8, the experimental total pressure drop data is plotted vs. the calculated value using the recommended correlation. The average error is −0.6% and the mean error is 6.0%.

In Table 4, the composite data base is subdivided into air/water and nonair/water systems. Average and mean absolute errors are indicated for each subset of data plus the entire composite data base. Three correlation techniques are compared. They are: this new correlation, Colwell's (1979), and Fair's (1963) correlations. The mean absolute error for the entire data base for this new correlation is about a factor of two less than the mean absolute error given by the other correlations. The average error of this new correlation is about 8% of the average error of the other correlations. The standard deviation of the new correlation is 7.8%.

ACKNOWLEDGMENTS

We would like to thank Dr. B. J. Savilonis (now at Worcester PolyTechnic Institute) and S. Welhoelter, M. Hoffman, A. Christensen, and M. Rensch of Widener University for obtaining part of the reported data. We would also like to thank Dr. J. M. Geist and Dr. K. B. Wilson of Air Products for their careful review and editorial comments.

NOTATION

a = constant in Eq. 2; according to Liebson, a equals 0.499
A_H = perforated area of tray (m^2)
A_T = total bubbling area of tray (m^2)
b = constant used in Eq. 9
c_V = discharge coefficient in Eq. 2
C = constant defined by Eq. 6b
C_1 = modified Francis weir coefficient defined by Eq. 5a
C_d = constant defined by Eq. 5c
C_D' = drag coefficient on a liquid droplet
C_F = Francis' weir constant
D_B = characteristic diameter of a bubble (m)

D_{Bmax} = departure bubble diameter from the sieve tray (m)
D_H = diameter of the tray perforation (m)
$f(\ )$ = functional operator of argument
g = acceleration due to gravity (m/s^2)
h = height of the fluid at the weir end (end ② of Figure A) (m)
h_D = dry hole pressure drop (m of liquid)
h_f = height of the fluid upstream of the weir (end ① of Figure A) (m)
h_{Fa} = observed froth height on the tray (m)
h_{Fe} = effective froth height defined in Eq. 6a (m)
h_g = hydraulic gradient due to the flow of froth over the tray (m of liquid)
h_L = height of the liquid inventory on the tray (m of liquid)
h_{Lonly} = liquid height on the tray if unaerated and no weeping occurs (m of liquid)
h_m = pressure drop measured by tray-mounted manometer for bubbling tray (m of liquid)
h_{ow} = crest height over the weir (m of liquid)
h_T = total pressure drop across the tray (m of liquid)
h_V = pressure drop due to the resistance of passage of gas through tray (m of liquid)
h_w = height of weir (m)
h_σ = pressure drop due to surface tension (m of liquid)
$h_{2\phi}$ = height of the predominately two-phase region on sieve tray (m)
$K_s = V_s \left(\frac{\rho_V}{\rho_L - \rho_V}\right)^{1/2}$ (m/s)
P_1 = pressure upstream of flow (at end ① of Figure A)
P_2 = pressure at weir end (at end ② of Figure A)
P_∞ = ambient pressure
P_B = pressure inside bubble (N/m^2)
P_L = pressure in liquid phase (N/m^2)
$\overline{\Delta P_B}$ = average pressure drop during growth of bubble (N/m^2)
$\dot{Q}$ = volumetric liquid flow rate (m^3/min)
$\dot{Q}_L$ = flow rate of liquid per unit length of weir (m^3/min·m)
r_B = radius of bubble (m)
r_D = radius of liquid droplet (m)
V_1 = velocity of approach of fluid to weir (end ① of Figure A)
V_2 = velocity of discharge of fluid over weir (end ② of Figure A)
V_H = vapor velocity through sieve perforations (m/s)
V_s = superficial vapor velocity based on total aerated area of plate (m/s)
W_B = total work required to generate the bubble (N·m)
z = length coordinate from bottom of tray (m)
β = aeration factor as defined by Fair
δ = liquid contained in droplet is δ fraction of the fluid which formed liquid membrane making up the bubble
θ = departure contact angle between bubble interphase and tray (degrees)
μ = liquid viscosity (N·s/m^2).
ξ_1 = length coordinate perpendicular to direction of flow (at end ① of Figure A)
ξ_2 = length coordinate perpendicular to direction of flow (at end ② of Figure A)
π_1, π_2 = as defined in Eq. 10c
ρ = density of fluid flowing over weir (kg/m^3)
ρ_L = density of liquid (kg/m^3)
ρ_V = density of vapor (kg/m^3)
$\rho_{2\phi}$ = density distribution function of froth (kg/m^3)
σ = surface tension (N/m)
ϕ = local value of $\rho_{2\phi}/\rho_L$
ϕ_a = relative froth density obtained from dividing h_L by observed froth height, h_L/h_{Fa}
ϕ_e = effective relative froth density defined in Eq. 6a

LITERATURE CITED

Azbel, D. S., "The Hydrodynamics of Bubbler Processes," *Int. Chem. Eng.*, **3**, (3), 319 (1963).
Bernard, J. D. T., and R. W. H. Sargent, "The Hydrodynamic Performance of a Sieve Plate Distillation Column," *Trans. Instn. Chem. Engrs.*, **44**, T314 (1966).
Bhavaraju, S. M., T. W. F. Russell, and H. W. Blanch, "The Design of Gas Sparged Devices for Viscous Layer Systems," *AIChE J.*, **24** (3), 454 (1978).
Billet, R., S. Conrad, and C. M. Grubb, "Some Aspects of the Choice of Distillation Equipment," *Int. Chem. Eng. Symp. Ser.*, **32**, 94 (1969).
Brambilla, A., G. Nardini, G. F. Nencetti, and S. Zanelli, "Hydrodynamic Behavior of Distillation Columns: Pressure Drop in Plate Distillation Columns," *Instn. Chem. Engrs. Symp. Ser.*, **32**, 2:58 (1969).
Colwell, C. J., "Clear Liquid Height and Froth Density on Sieve Trays," AIChE Meeting, San Francisco (Nov., 1979). *Ind. Eng. Chem. Process Des. Dev.*, **20** (2), (1981).
Fair, J. R., in B. D. Smith, *Design of Equilibrium Stage Processes*, McGraw-Hill (1963).
Foss, A. S., and J. A. Gerster, "Liquid Film Efficiencies on Sieve Trays," *Chem. Eng. Prog.*, **52**, 29-J (1956).
Friend, L., E. J. Lemieux, and W. C. Schreiner, "New Data on Entrainment from Perforated Trays at Close Spacings," *Chem. Eng.*, 101 (Oct., 1960).
Gilbert, T. J., "Liquid Mixing on Bubble-Cap and Sieve Plates," *Chem. Eng. Sci.*, **10**, 243 (1959).
Harris, I. J., and G. H. Roper, "Performance Characteristics of a 12-in. Diameter Sieve Plate," *Can. J. of Chem. Eng.*, **40**, 245 (1962).
Hutchinson, M. H., A. G. Buron, and B. P. Miller, "Aerated Flow Principle Applied to Sieve Plates," AIChE Meeting, Los Angeles (May, 1949).
Jones, D. W., and J. W. Jones, "Tray Performance Evaluation," *Chem. Eng. Prog.*, **71** (6), 65 (1975).
Kemp, H. S., and C. Pyle, "Hydraulic Gradient Accross Various Bubble-Cap Plates," *Chem. Eng. Prog.*, **45** (7), 435 (1949).
Kim, S. K., "Theoretical Study of Vapor-Liquid Hold-up on a Perforated Plate," *Int. Chem. Eng.*, **6** (4), 634 (1966).
Kuehler, G. P., and M. Van Winkle, "Effect of Vapor Rate and Weir Height on Foaming," *J. of Chem. Eng. Data*, **14** (2), 225 (1969).
Lemieux, E. J., and L. J. Scotti, "Perforated Tray Performance," *Chem. Eng. Prog.*, **65** (3), 52 (1969).
Liebson, I., R. E. Kelley, and L. A. Bullington, "How to Design Perforated Trays," *Petrol. Ref.*, **36** (2), 127 (1957).
Mayfield, F. D., W. L. Church, A. C. Green, and R. W. Rasmussen, "Perforated-Plate Distillation Columns," *Ind. Eng. Chem.*, **44** (9), 2238 (1952).
Nutter, D. E., "Ammonia Stripping Efficiency Studies," *AIChE Symp. Ser.*, **68** (124), 73 (1971).
Nutter, D. E., "Weeping and Entrainment Studies for Sieve and V-Grid® Trays in An Air-Oil System," Third Int. Symp. on Distillation, *Int. Chem. Eng. Symp. Ser.*, **56**, 3.2/47 (1979).
Pavlov, V. P., "Determination of the Total Resistance of a Bubbler Sieve Plate," *Int. Chem. Eng.*, **4** (4), 680 (1964).
Rehbock, T., in "Precise Weir Measurements," by E. W. Schoder and K. B. Turner, *Trans. ASCE*, **93**, 1147 (1929).
Robinson, C. S., and E. R. Gilliland, *Elements of Fractional Distillation*, McGraw-Hill, New York (1950).
Sakata, M., and T. Yanagi, "Performance of a Commercial Sieve Tray," Third Int. Symp. on Distillation, *Int. Chem. Eng. Symp. Ser.*, **56**, 3.2/21 (1979).
Sargent, R. W. H., J. D. T. Bernard, W. P. MacMillan, and R. C. Schroter, "The Performance of Sieve Plates in Distillation," Proceedings of the Symp. on Distillation, 81 (1964).
Sterbacek, Z., "Hydrodynamics of Perforated Trays with Downcomers," *British Chem. Eng.*, **12** (10), 1577 (1967).
Thomas, W. J., and O. Ogboja, "Hydraulic Studies in Sieve Tray Columns," *Ind. Eng. Chem. Process Des. Develop.*, **17** (4), 429 (1978).

APPENDIX: ANALYSIS TO CALCULATE CREST OVER A WEIR FOR A UNIFORM DENSITY FLUID

A schematic of the flow over a rectangular weir is shown in Figure A. The control volume is illustrated. The inlet is denoted by subscript 1 and the weir end by subscript 2. It is assumed that the volumetric flow rate at ① and ② are equal. A uniform inlet velocity is assumed, however, the approach could be generalized to account for a specified initial velocity distribution. The static

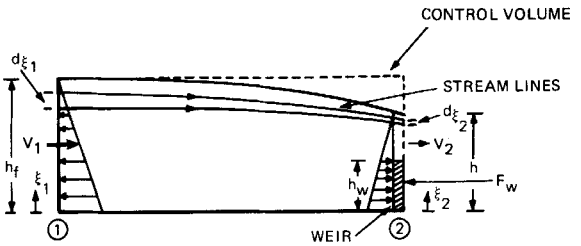

Figure A. Definition of symbols for flow over weir calculation.

pressure at the inlet of the control volume is given by the following,

$$\frac{P_1}{\rho} + g\xi_1 = \frac{P_\infty}{\rho} + gh_f. \tag{A1}$$

Just outside the exit weir, the fluid is free falling, therefore, if the effect of streamline curvature at the outlet end of the control volume is assumed small, It can be assumed that the static pressure opposing the fluid flow just outside of the exit weir is equal to the ambient pressure.

Substituting Eq. A1 into the Bernoulli equation for a streamline,

$$V_2^2 = V_1^2 + 2g(h_f - \xi_2) \tag{A2}$$

The equation of continuity is:

$$\dot{Q}_L = \int_{h_w}^{h} V_2 d\xi_2 = V_1 h_f \tag{A3}$$

Substitution of Eq. A2 into Eq. A3 and then integrating gives:

$$h_f = \frac{V_1^2}{3g}\left[\left\{1 + \frac{2g}{V_1^2}(h_f - h_w)\right\}^{3/2} - \left\{1 + \frac{2g}{V_1^2}((h_f - h)\right\}^{3/2}\right] \tag{A4}$$

To write a momentum balance over the control volume, the force on the weir, F_w, must be determined. Two cases are considered which should bound the actual force on the weir. In the first case, it is assumed that the force due to froth impact on the weir is negligible. In the second case, the froth is assumed to impact on the exit weir. For both cases, the hydrostatic load on the exit weir is calculated based on the indicated trapezoidal profile.

For the first case, a momentum balance gives:

$$-\int_1 V_1^2 d\xi_1 + \int_2 V_2^2 d\xi_2 = \frac{gh_f^2}{2} - g\int_0^{h_w} (h - \xi_2) d\xi_2. \tag{A5}$$

As before, the effect of streamline curvature at the weir end is assumed negligible. Substitution of Eq. A2 into Eq. A5 and integrating gives:

$$h^2 - h\left[\frac{V_1^2}{g} + 2h_f + h_w\right] + \frac{V_1^2}{g}(h_f + h_w) + \left(\frac{h_f^2 - h_w^2}{2}\right) + 2h_f h_w = 0 \tag{A6}$$

For a given weir height h_w and flow rate $\dot{Q}_L$, Eqs. A3, A4 and A6 can be solved to calculate h_f, h, and V_1. The iterative technique used to solve these sets of equations is:

a. Guess a value of h_f (may be calculated from the Francis weir equation).

b. Calculate V_1 from Eq. A3.

c. Calculate h from Eq. A6. This is a quadratic equation, therefore, h is calculated without an additional iteration.

d. The values of h_f and h are substituted in the righthand side of Eq. A4 and a new value of h_f is calculated.

e. If the new value of h_f agrees with the guessed value, the iteration is complete, otherwise, steps b through d are repeated with the new calculated value of h_f until agreement between two successive calculations is obtained.

For Case 2, the force on the exit weir is assumed to equal hydrostatic load plus the impact load. P_2 at the weir is calculated from the Bernoulli equation assuming complete deceleration:

$$\frac{(P_2 - P_\infty)}{\rho} = \left[\frac{V_1^2}{2} + g(h_f - \xi_2)\right] \text{ for } 0 < \xi_2 < h_w \tag{A7}$$

From the momentum balance over the control volume,

$$h^2 - h\left(\frac{V_1^2}{g} + 2h_f\right) + \frac{V_1^2}{g}\left(h_f + \frac{h_w}{2}\right) + \left(\frac{h_f^2 - h_w^2}{2}\right) + h_f h_w = 0 \tag{A8}$$

The continuity Eqs. A3 and A4 are still applicable. Therefore, for Case 2, Eqs. A3, A4 and A8 can be solved for h_f, h, and V_1, for the specified values of $\dot{Q}_L$ and h_w. The iterative technique used for the solution is the same as for Eqs. A3, A4 and A6.

Manuscript received September 14, 1981; revision received May 10, and accepted May 28, 1982.